Asian Journal of Chemistry; Vol. 33, No. 5 (2021), 1099-1106

ASIAN JOURNAL OF CHEMISTRY

https://doi.org/10.14233/ajchem.2021.23086

Synthesis, Spectroscopic Studies, Antimicrobial Activity and Computational Calculations on 3-Nitroanilinium Dihydrogen Phosphate

SUBRAMANIAN THANGARASU[1,2,*], VADIVEL SIVA[1,2], SHUNMUGANARAYANAN ATHIMOOLAM[3] and SULTAN ASATH BAHADUR[1,2]

[1]Department of Physics, School of Advanced Sciences, Kalasalingam Academy of Research and Education, Krishnankoil-626126, India
[2]Condensed Matter Physics Laboratory, International Research Centre, Kalasalingam Academy of Research and Education, Krishnankoil-626126, India
[3]Department of Physics, University College of Engineering Nagercoil, Nagercoil-629004, India

*Corresponding author: E-mail: sthangarasu@gmail.com

Received: 3 December 2020; *Accepted*: 8 March 2021; *Published online*: 16 April 2021; AJC-20330

3-Nitroanilinium dihydrogen phosphate (3NADP) has been synthesized and crystallized successfully using the method of solvent evaporation solution growth. The molecular structure has been optimized and geometrical parameters of 3NADP also have been analyzed using B3LYP function with density functional theory (DFT) and Hartree-Fock (HF) methods with a 6-311++G(d,p) basis set. The comparison between computed vibrational spectra and experimental result shows an appreciable agreement. The thermal stability of 3NADP crystal was analyzed using TG/DTA and the melting point was identified at 209 ºC. The properties like electronegativity, chemical hardness, electrophilicity index and chemical potential of the crystal were determined through HOMO-LUMO study. Lower band gap value obtained in frontier molecular orbital analysis and favours the possible biological activity of 3NADP. The grown crystals was also screened for the antimicrobial activity against some specific potentially threatening microbes.

Keywords: 3-Nitroanilinium dihydrogen phosphate, Vibrational analysis, Antimicrobial activity, Population analysis.

INTRODUCTION

In push-pull molecule is like *m*-nitroaniline, intramolecular charge transfer (ICT) from the electron-donor (-NH_2) group to electron-acceptor (-NO_2) group through the phenyl ring. The optical non-linearity property determined by the method of experiment and computation on *m*-nitroaniline and *p*-nitroaniline [1-3]. 3-Nitroaniline and its derivatives are biologically important compounds involves in producing the significant hypoglycemic and antihyperglycemic effects in normal and alloxan-induced diabetic rabbits [4]. Also, 3-nitroaniline has a considerable chemical and pharmacological importance, because it plays a vital role in some biological processes. The organic protonation molecule relations between acceptors and donors holding N, O and S atoms were used in various medicines. A limited physicist have studied the donor molecules with electron delocalization potential with charge transfer molecules. The overlap of π-orbitals in the donor molecules leads to electron delocalization of the protonated from the amine families [5-8].

The aim of the work is to discover organic-inorganic crystal with the biological importance along with good physical, chemical and thermal properties is proposed. Based on the above precise details, 3-nitroaniline was treated with orthophosphoric acid and the crystals of 3-nitroanilinium dihydrogen phosphate (3NADP) were grown. The synthesis, structural, spectroscopic, thermal and antimicrobial analyses of 3NADP are reported in this article.

EXPERIMENTAL

3-Nitroanilinium dihydrogen phosphate (3NADP) was synthesized from 3-nitroaniline (AR grade, HiMedia Fine Chemicals, India) and orthophosphoric acid (AR grade). The acetone was used to dissolve the chemicals and the solution was stirred for 1 h using a magnetic stirrer. The reaction was permitted at room temperature to happen and the compound 3-nitroanilinium dihydrogen phosphate was obtained (**Scheme-I**). However, the desired quality of single crystal of 3NADP growth was not obtained even after several attempts.

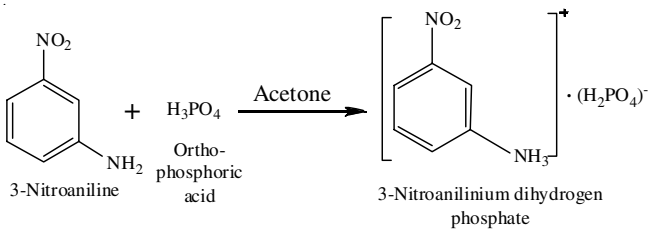

Scheme-I: Synthetic route of 3-nitroanilinium dihydrogen phosphate (3NADP)

So powder X-ray diffraction confirms the new phase of 3-nitroanilinium dihydrogen phosphate.

Characterization: The powder XRD study of grown crystal of 3NADP carried out by Bruker X-ray diffractometer (D8 advanced ECO XRD system) with SSD160 1D detector in the range of 0º to 80º (2θ). The DASH 3.3.2 program [9] used to collect preliminary data of 3NADP was calculated and the strong intensity peaks indexed. The Nexus 670 FTIR spectrometer is used to make infrared spectral measurements of grown crystal which is in the range of 4000-400 cm^{-1} using KBr pellet. The FT-Raman spectra of the grown crystal was recorded in the BRUKER RFS 27 using Nd:YAG laser source and operated at 1064 nm in the range of 4000-400 cm^{-1} with the resolution ~1-2 cm^{-1}.The thermal analyses (TG/DTA) of 3NADP was conducted using SII (SEIKO), TG/DTA-6200, Japan using air atmosphere at the range of 20 ºC/min.

Computational quantum chemical analysis: The efficient quantum mechanical calculations were carried out by Hartree-Fock (HF) method and Density Functional Theory (DFT) and the molecular structure was optimized with 6-311++G(d,p) basis set. Intel Core i5/3.20 GHz computer with Gaussian 09W [10] program package used for computational analysis. The accepted approach is HF and DFT method for the computation of molecular structure and vibrational frequencies with the three-parameter hybrid function (B3) for the exchange part and the Lee–Yang–Parr (LYP) correlation function [11-13]. The principle of statistical mechanics used for thermodynamic property calculation and vibrational frequencies (normal mode), which gives the details about title compound in gas phase. The vibrational frequency assignments were calculated using GAUSSVIEW program [14] with symmetry considerations. The electronic properties, such as HOMO-LUMO energies were calculated and computed by the HF and DFT methods.

RESULTS AND DISCUSSION

Structural analysis: The unit cell parameters of grown crystal of 3-nitroanilinium dihydrogen phosphate (3NADP) were analyzed and the values are given in Table-1. The powder XRD patterns and predicted unit cell values confirmed the salt formation. The XRD pattern of the grown crystal 3NADP was compared with 3-nitroaniline (Fig. 1). It is clearly observed that few new intensity peaks appeared in 3NADP crystals and appeared as monoclinic system.

The asymmetric part of both unit cells contains 3-nitroaniline cation and the charge neutrality is attained with dihydrogen phosphate anion in 3NADP. The optimized structure of 3-nitroanilinium dihydrogen phosphate with atom numbering is shown in Fig. 2, while the bond length and bond angle values are listed in Table-2. In H-F level, the C–C bond length of the phenyl ring was in the range of 1.377-1.3926 Å [15,16], while in B3LYP level, the C–C bond length was 1.389-1.401 Å. In phosphate anion, the optimized P=O bond length was found to be 1.455 Å at H-F method and 1.487 Å at B3LYP method. Similarly, the optimized P–O bond lengths were around 1.566-1.569 Å [17] at HF method and 1.589-1.609 Å at B3LYP method.

TABLE-1
STRUCTURAL PARAMETERS FOR 3NADP

Unit cell parameters	Values
a (Å)	8.966 (8)
b (Å)	4.500 (2)
c (Å)	8.707 (6)
α (°)	90
β (°)	90.5
γ (°)	90
Volume	351.2

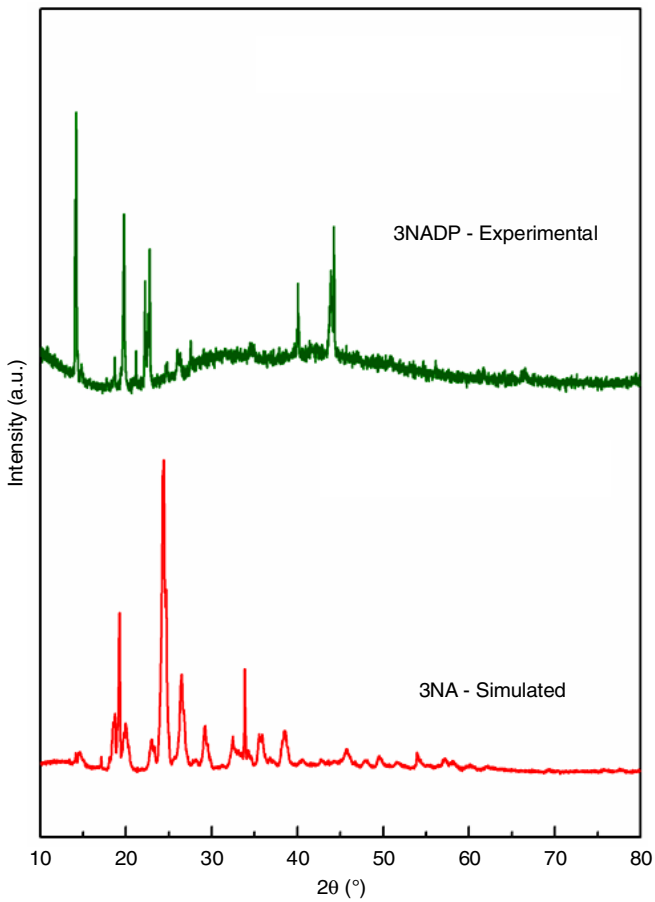

Fig. 1. XRD pattern for 3-nitroanilinium dihydrogen phosphate (3NADP)

Mulliken charge analysis: The histogram of atomic charges of 3NADP is shown in Fig. 3 and computed charge values are given in Table-3. In general, Mulliken population analysis has an important role in the molecular system because atomic charges affect dipole moment, polarizability and electronic structure in the quantum chemical calculations [18]. The phosphorus atom is surrounded by four electronegative oxygen atoms, which makes it more electropositive (0.806e in HF and

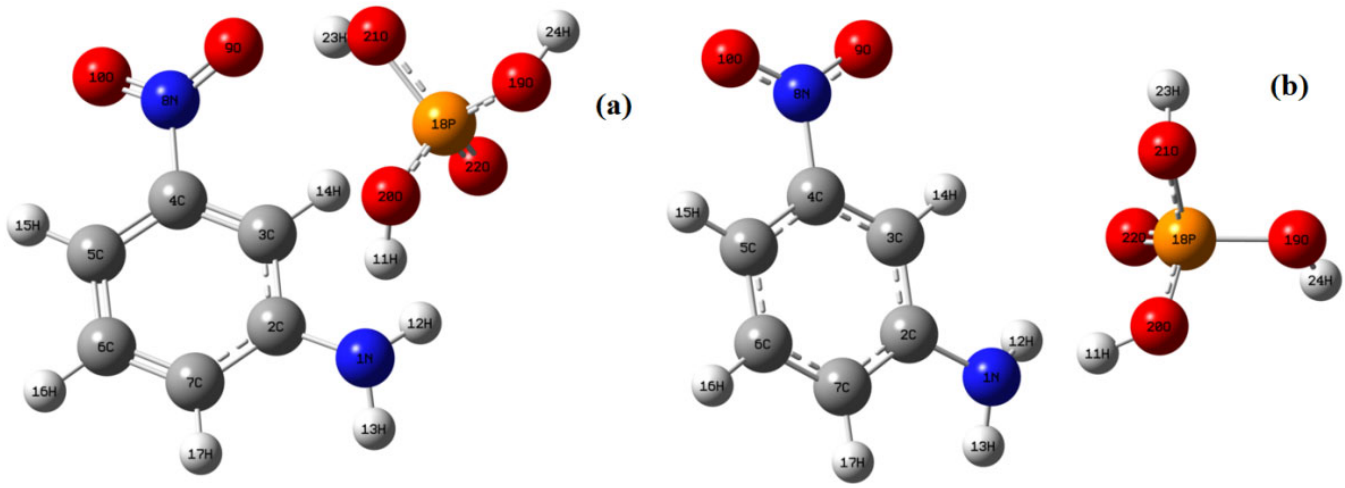

Fig. 2. Optimized geometry of 3NADP by (a) HF and (b) B3LYP method

TABLE-2
OPTIMIZED MOLECULAR GEOMETRICAL PARAMETERS

Bond length (Å)			Bond angle (°)		
Geometrical parameters	HF/6-311++(d,p)	B3LYP/6-311++(d,p)	Geometrical parameters	HF/6-311++(d,p)	B3LYP/6-311++(d,p)
N1–C2	1.398	1.413	N1–C2–C3	119.5	119.9
C4–N8	1.466	1.483	N1–C2–C7	121.6	120.8
C2–C3	1.388	1.398	C3–C4–N8	117.4	118.2
C2–C7	1.393	1.401	C5–C4–N8	119.1	118.8
C3–C4	1.377	1.389	C3–C2–C7	118.7	119.3
C4–C5	1.378	1.390	C2–C3–C4	119.0	118.7
C5–C6	1.385	1.392	C3–C4–C5	123.5	123.0
C6–C7	1.383	1.392	C4–C5–C6	116.9	117.6
N8–O9	1.196	1.225	C5–C6–C7	121.1	120.8
N8–O10	1.181	1.224	C2–C7–C6	120.7	120.6
P18–O19	1.567	1.608	C4–N8–O9	117.4	117.8
P18–O20	1.566	1.589	C4–N8–O10	118.1	117.6
P18–O21	1.569	1.602	O9–O8–O10	124.5	124.6
P18–O22	1.455	1.487	O19–P18–O20	101.7	105.0
			O19–P18–O21	102.3	101.4
			O19–P18–O22	117.0	115.1
			O20–P18–O21	106.8	102.9
			O20–P18–O22	113.4	114.6
			O21–P18–O22	114.2	116.2

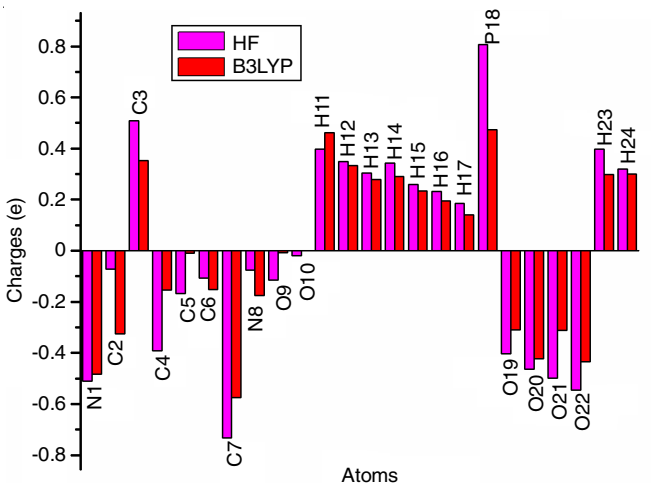

Fig. 3. Histogram of atomic charges on 3NADP by HF and B3LYP methods

TABLE-3
COMPUTED ATOMIC CHARGES OF 3NADP

Atoms connected	HF/6-311++ G(d,p)	B3LYP/6-311++ G(d,p)	Atoms connected	HF/6-311++ G(d,p)	B3LYP/6-311++ G(d,p)
N1	-0.512	-0.482	H13	0.304	0.279
C2	-0.072	-0.325	H14	0.343	0.290
C3	0.509	0.353	H15	0.260	0.234
C4	-0.391	-0.153	H16	0.233	0.194
C5	-0.168	-0.010	H17	0.186	0.140
C6	-0.107	-0.151	P18	0.806	0.474
C7	-0.732	-0.575	O19	-0.404	-0.310
N8	-0.076	-0.176	O20	-0.463	-0.422
O9	-0.116	-0.008	O21	-0.499	-0.311
O10	-0.020	-0.001	O22	-0.545	-0.435
H11	0.398	0.463	H23	0.398	0.299
H12	0.349	0.333	H24	0.320	0.300

0.474e in B3LYP) and the carbon atom (C7) has more electronegativity (-0.732e in HF and -0.575e in B3LYP), as it is surrounded by one hydrogen atom (H17) and two electronegative carbon atoms (C2 and C6).

Vibrational analysis: 3-Nitroanilinium dihydrogen phosphate molecule consists of 24 atoms, hence undergoes 66 normal modes of vibrations. In 3NADP, the experimental spectra (FT-IR and FT-Raman) are compared with their theoretical counterparts as shown in Fig. 4. The observed and computed frequencies of 3NADP with their vibrational assignments are given in Table-4.

Vibrations of –NH_2 group: The NH_2 antisymmetric stretching vibration is scaled at 4027 cm^{-1} in HF and 3592 cm^{-1} in B3LYP levels as mode 64 [19,20]. Similarly, NH_2 symmetric

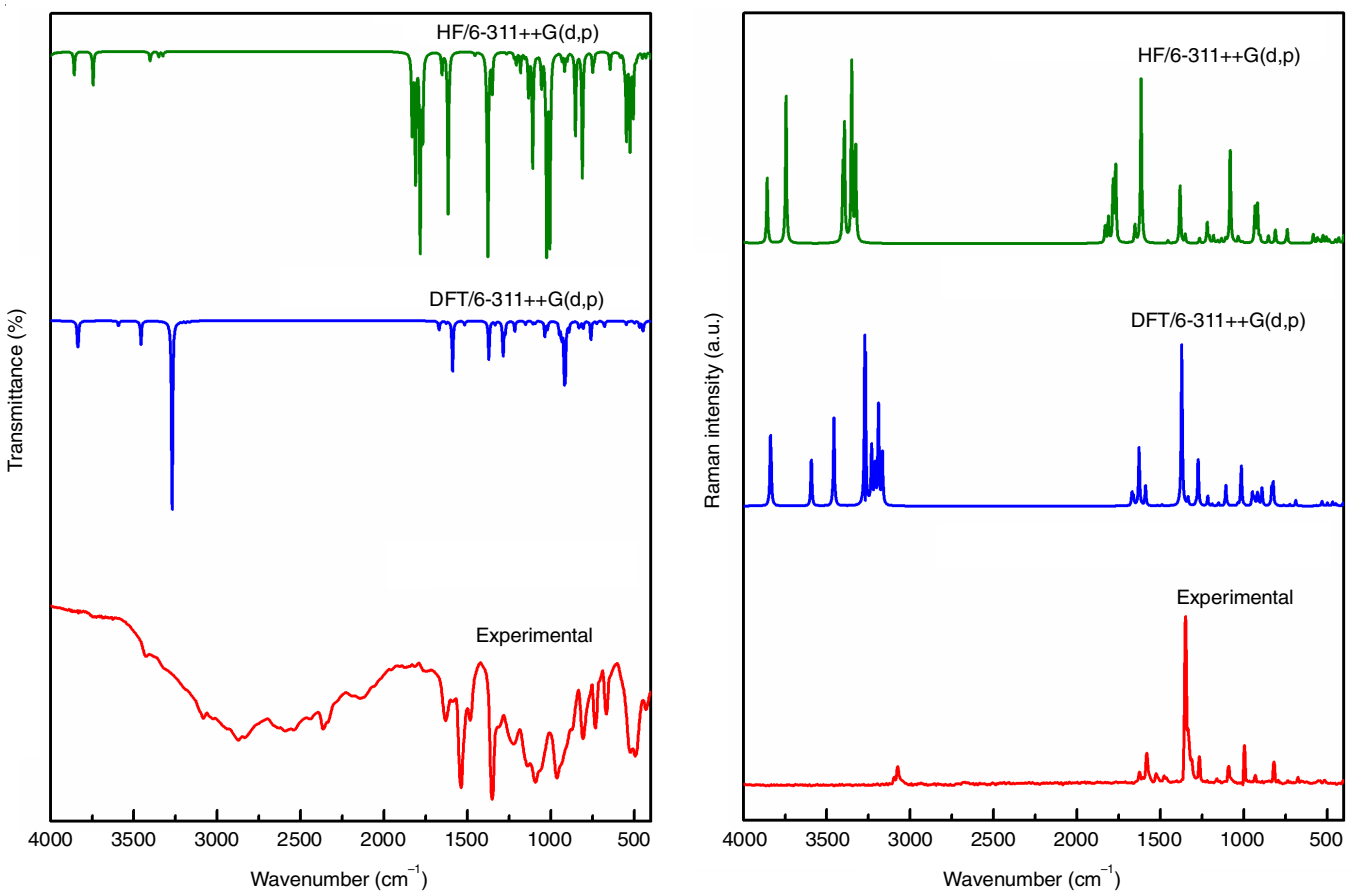

Fig. 4. Experimental and computed FT-IR and Raman spectra of 3-nitroanilinium dihydrogen phosphate (3NADP)

TABLE-4
EXPERIMENTAL (FT-IR AND FT-RAMAN) AND COMPUTED FREQUENCIES OF 3-NITROANILINIUM DIHYDROGEN PHOSPHATE (3NADP) WITH THEIR VIBRATIONAL ASSIGNMENTS

Mode No.	Observed frequency (cm^{-1})		Calculated frequency (cm^{-1})						Vibrational assignments
			HF			B3LYP			
	IR	Raman	ν_{cal}	$^aI^{IR}$	$^bI^{Raman}$	ν_{cal}	$^aI^{IR}$	$^bI^{Raman}$	
1			36	2.436	1.213	10	0.911	0.3881	Lattice vibration
2			43	0.365	2.482	30	0.240	3.9404	Lattice vibration
3			57	4.609	0.386	37	0.219	2.0123	γ(P–OH) + t NH_2
4			73	0.918	0.690	48	1.133	0.5952	γ(P–OH) + t NH_2
5			86	0.849	0.281	59	1.406	0.6042	γ(P–OH)
6			98	11.200	2.682	109	14.338	0.4282	β(P–OH)
7			102	6.751	0.263	145	2.762	2.523	β(P–OH)
8			187	3.691	2.042	151	73.777	2.9411	γ(P–OH)
9			197	98.999	1.871	170	4.036	1.776	Lattice vibration
10			240	2.673	0.407	223	2.210	0.778	ρ(NO_2+ NH_2)
11			258	2.284	0.892	250	28.425	0.6703	γ(P–OH + C–H)
12			337	13.891	0.755	270	63.372	1.4262	γ(P–OH)
13			392	17.779	0.197	362	77.371	0.3489	γ(P–OH)
14			400	8.031	2.972	369	29.027	1.0574	γ(P–OH)
15			430	10.149	2.072	375	6.060	3.8039	ρ(NO_2+ NH_2) + β(C–N)

16			451	10.205	1.384	405	0.834	2.4349	$\rho(NO_2+ NH_2) + \beta(C–N+ C–C)$
17			480	4.205	0.337	435	5.253	0.5778	$\gamma(C–H + C–C)$
18			489	10.996	1.200	445	47.875	0.7857	ωPO_2
19			505	117.219	2.307	449	49.071	1.5937	$\gamma(P–OH) + \delta(COO(H))$
20	518 m		524	132.250	1.129	467	44.287	3.2923	$\rho PO_2+ \delta(COO(H))$
21			525	49.402	1.891	498	15.855	2.6716	$t (NH_2)$
22			547	162.326	1.087	530	4.788	3.9217	$t (NH_2) + \gamma(C–H)$
23			558	17.319	2.026	547	26.801	0.3385	$t (NH_2) + \gamma(C–H)$
24			583	7.094	3.354	563	1.563	0.6097	$\beta(C–H + C–C)$
25	668 m		645	33.498	0.261	678	40.403	0.2237	$\gamma(C–H)$
26			739	12.508	5.356	688	5.121	4.7194	$\beta(C–H + C–C)$
27	736 m		748	36.145	0.739	724	19.573	1.6683	$\beta(C–H + C–C + C–N)$
28	817 m	806 w	810	237.752	5.366	759	140.107	1.1258	$\omega(NO_2+ NH_2) + \gamma(P–OH)$
29			852	156.293	3.086	806	53.516	0.5175	$\gamma(C–H)$
30			902	12.851	2.097	823	30.993	18.5374	$\nu(P–O)$
31			917	33.240	15.352	832	44.500	14.7678	$\delta(NO_2) + \nu(C–N)$
32			933	14.155	14.302	890	65.757	15.4673	$\omega(NH_2)$
33		1002 w	1005	356.176	0.491	912	348.247	6.3244	$\gamma(C–H) + \omega(NH_2)$
34			1015	8.070	0.358	918	369.138	9.3586	$\gamma(C–H) + \omega(NH_2)$
35			1025	373.655	0.514	933	88.311	0.9458	$\gamma(C–H) + \nu(P–O)$
36			1033	7.593	2.617	937	56.059	6.1962	$\nu_s(P=O)$
37			1055	61.677	0.139	948	85.716	11.3612	$\gamma(C–H) + \omega(NH_2)$
38	978 m	1093 w	1081	3.640	38.659	993	0.175	0.2379	$\gamma(C–H)$
39			1105	8.646	0.095	1014	1.677	34.6925	$\beta(C– C)$
40			1108	210.007	1.685	1020	59.025	1.7633	$\nu_{as}(P=O)$
41			1133	80.869	1.896	1035	113.939	1.8275	$\nu(P=O)$
42	1105 m		1156	7.942	1.244	1094	19.621	0.7223	$t (NH_2) + \beta(C–H)$
43			1181	37.348	3.405	1107	20.524	18.8381	$\beta(C–H + C–C) + \nu(C–N)$
44	1232 w		1206	23.275	2.584	1151	26.962	3.2372	$t (NH_2)$
45			1219	10.604	8.910	1190	0.301	2.0725	$\beta(C–H)$
46		1278 w	1265	3.789	2.333	1216	78.350	9.3159	$\nu_{as}(PO_2)$
47	1359 s	1335 s	1351	70.980	3.868	1273	80.624	42.8263	$\beta(C–H + C–C) + \nu(C–N)$
48			1376	360.247	1.750	1286	261.987	1.7845	$\beta(P–OH)$
49			1382	77.689	24.843	1334	25.728	7.6585	$\beta(C–H)$
50			1454	6.341	1.449	1369	55.046	6.8614	$\nu(C–C) + t (NH_2)$
51	1542 s		1614	122.483	36.936	1371	244.320	148.6699	$\nu(C–N) + \nu_s (NO_2)$
52			1615	185.699	40.449	1491	1.254	1.6316	$\nu(C–C)$
53	1647 m	1566 w	1652	39.665	8.172	1516	28.938	0.7044	$\nu(C–C)$
54			1768	147.995	36.840	1588	381.639	20.2657	$\nu_{as}(NO_2) + \nu(C–C)$
55			1783	368.051	29.196	1627	16.765	58.9829	$\nu(C–C) + \beta(N–H)$
56			1811	238.466	12.535	1660	4.844	8.4825	$\delta(NH_2) + \nu(C–C)$
57			1831	149.877	8.120	1670	66.924	13.5486	$\delta(NH_2)$
58		3085 w	3326	7.911	66.609	3166	8.532	76.0192	$\nu(C–H)$
59			3350	9.756	128.273	3190	9.102	148.5519	$\nu(C–H)$
60			3394	1.907	78.409	3211	5.554	56.8921	$\nu(C–H)$
61			3402	17.171	44.517	3231	6.271	86.4456	$\nu(C–H)$
62			3744	62.956	116.620	3270	1425.156	303.9283	$\nu(O–H)$
63			3857	43.739	53.212	3457	179.097	139.4773	$\nu_s (NH_2)$
64			4027	281.231	37.110	3592	36.361	76.1176	$\nu_{as} (NH_2)$
65			4055	571.877	89.273	3833	136.838	51.3028	$\nu(O–H)$
66			4164	200.715	65.037	3838	115.830	99.0362	$\nu(O–H)$

vs = very strong; m = medium; w =weak; ν_{as} = asym. stretching; ν_s = sym. stretching; γ = out-of-plane bending; β = in-plane bending; ρ = rocking; δ = scissoring; t = twisting; ω = wagging.

stretching vibration is computed at 3857 and 3457 cm^{-1} in HF and DFT/B3LYP levels (mode 63), respectively. The NH_2 scissoring is calculated at 1831 cm^{-1} in HF and 1670 cm^{-1} in B3LYP methods (mode 57). The NH_2 twisting vibration is computed at 1454 cm^{1} in HF and 1369 cm^{-1} in B3LYP methods (mode 50). The NH_2 wagging vibrations is calculated at 1055 and 948 cm^{-1} in HF and B3LYP levels (mode 37), respectively. The NH_2 and NO_2 rocking vibrations are computed at 451 and 405 cm^{-1} in HF and B3LYP levels (mode 16), respectively. Also, these peaks are not observed in the experimental spectra.

Vibrations of –NO_2 group: The NO_2 group asymmetric and symmetric stretching vibrations representing the bands around 1570-1500 cm^{-1} and 1370-1300 cm^{-1} for nitrobenzene and its substituted compounds, respectively. The NO_2 asymmetric stretching vibrations at 1770 and 1589 cm^{-1} was computed by HF and B3LYP methods, respectively. The NO_2 symmetric stretching vibrations are theoretically found by HF at 1574 and B3LYP at 1371 cm^{-1} (mode 49), respectively.

C–C and C–N vibrations: The region around 1600-1300 cm^{-1} represents the C–C and C–N stretching vibrations. A medium intensity peak at 1647 cm^{-1} in FT-IR spectrum, while the weak peak at 1566 cm^{-1} in FT-Raman spectrum was assigned to C–N stretching vibrations and both are computed at 1652 and 1516 cm^{-1} in HF and DFT/B3LYP levels (mode 53), respectively. Apart from this, some more mode 56, mode 55 and mode 52 also represented the C–C stretching vibrations [21-23]. A strong peak observed at 1542 cm^{-1} in FT-IR spectrum and calculated at 1614 and 1371 cm^{-1} in HF and DFT/B3LYP levels (mode 51), respectively.

Vibration of C-H group: The C–H stretching vibrations occurred in the characteristic region around 3100 cm^{-1} and also represented the aromatic structure of the 3NADP and observed as a weak peak at 3085 cm^{-1} in FT-Raman spectrum [24]. The stretching vibrations were calculated by HF and B3LYP levels at 3402-3166 cm^{-1} (mode 58 to mode 62). The in-plane bending and out-plane bending vibrations of aromatic C–H represent the band around of 1300-1100 and 1100-900 cm^{-1}, respectively. The C–H in-plane bending vibration of 3NADP was observed as a strong peak at 1359 and 1335 cm^{-1} in FT-IR and FT-Raman spectrum, respectively. The observed wavenumbers are well matched with the calculated wavenumbers by HF and DFT/B3LYP levels (mode 47). The out-plane bending C–H vibration theoretically computed at 1055 cm^{-1} in HF and 948 cm^{-1} in B3LYP levels (mode 37).

Vibrations of dihydrogen phosphate anion: In 3NADP, the O–H stretching vibrations are calculated in the range of 4164-3270 cm^{-1} (mode 66, mode 65 and mode 62) by HF and DFT/B3LYP calculations. The P=O stretching mode theoretically calculated and predict the vibration at 1133 cm^{-1} in HF and 1035 cm^{-1} in DFT/B3LYP calculations (mode 41). The PO_2 asymmetric stretching modes are observed at 1278 cm^{-1} as a weak peak in Raman spectrum. These values are good in match with the theoretical calculations predict the mode 46. The P=O asymmetric stretching is theoretically calculated at 1108 and 1020 cm^{-1} (mode 40) in HF and DFT/B3LYP levels, respectively. The calculated values of P=O symmetric stretchings by HF and DFT/B3LYP calculations was found to be at 1033 and 937 cm^{-1} (mode 36). The medium intensity band at 518 cm^{-1} in FT-IR spectrum assigned to PO_2 rocking mode. These experimental results were good in agreement with the theoretical calculations. Also, the mode 20 and mode 13 represents the PO_2 wagging mode.

Frontier molecular orbital analysis: Frontier molecular orbital analysis was used to calculate electric and optical properties of organic molecules. The calculated HOMO, LUMO energies and the related parameters of 3NADP were calculated by HF and B3LYP methods are given in Table-5 and the energy level diagrams are shown in Fig. 5. The small frontier orbital energy gap is associated with a high chemical reactivity because a huge amount of charge transfer occurred within the molecules. The large charge transfer and small energy gap and influences the bioactivity of 3NADP. Around 400 energy levels were observed for 3NADP in the energy ranges of -80.115 au to 166.50 au and -77.217 au to 163.356 au in HF and B3LYP methods, respectively. The calculated HOMO and LUMO energy values of 3NADP molecule in HF and B3LYP level are –0.338/0.029 a.u. and –0.258/–0.106 a.u. The energy gap value between the frontier orbital was 0.367 a.u. in HF and 0.152 a.u. in B3LYP level.

Thermal studies: The thermal behaviour of 3NADP was studied in the temperature range of 40-650 ºC in air atmosphere using simultaneous TG/DTA analysis. The TG/DTA curve (Fig. 6)

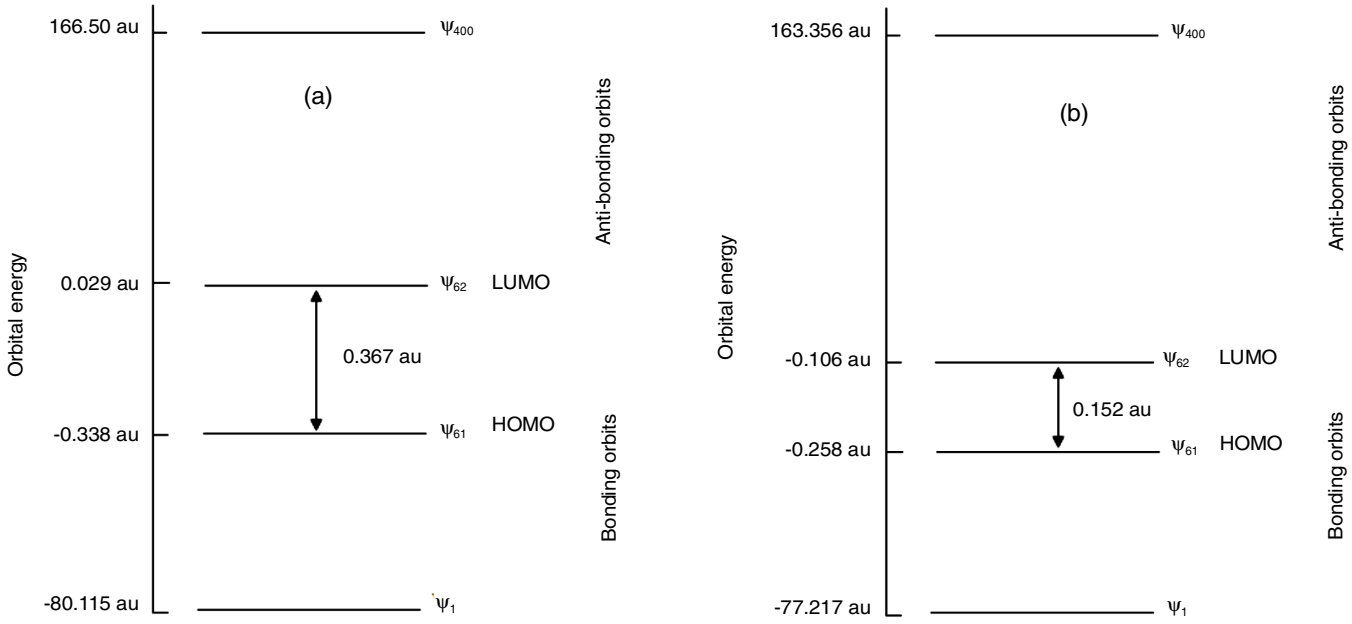

Fig. 5. Molecular orbital energy level diagram by (a) HF and (b) B3LYP levels

TABLE-5
CALCULATED ENERGY VALUES OF 3NADP

Parameters (a.u.)	HF/6-311++G(d,p)	B3LYP/6-311++G(d,p)
E_{LUMO}	0.029	-0.106
E_{HOMO}	-0.338	-0.258
$\Delta(E_{LUMO} - E_{HOMO})$	0.367	0.152
Electron affinity (A)	-0.029	0.106
Ionization potential (I)	0.338	0.258
Chemical hardness (η)	0.184	0.076
Chemical potential (μ)	-0.155	-0.182
Electronegativity (χ)	0.155	0.182
Electrophilicity index	0.065	0.218

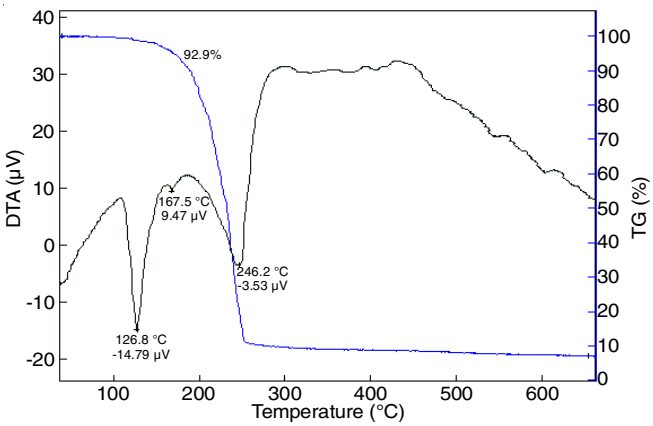

Fig. 6. TG/DTA curve of 3-nitroanilinium dihydrogen phosphate (3NADP)

represents that the decomposition in the range of 246.2-650 ºC. The decomposition of 3NADP occurs in three main steps within temperature range as shown Fig. 7. The first step of decomposition in the temperature range of 150-190 ºC as observed in weight loss 12% due to the removal of water group from the present compound. The second step in the temperature range of 190-210 ºC major weight loss 41% owing to removal of NO and PH_3 from the earlier intermediate compound. The third step is observed in the temperature range of 210-220 ºC with the weight loss of 26% owing to the removal of CO. The two weak endothermic peaks observed at 126.8 and 167.5 ºC were due to the loss of lattice water molecules. The melting point of the compound (endothermic peak) was observed at 246.2 ºC.

Antimicrobial activity: The antibacterial activity of the 3NADP crystal was studied against *Klebsiella pneumoniae* (Gram-negative), *Staphylococcus aureus* (Gram-positive) and *Candida albicans* (antifungal) using disc diffusion method [25]. The bacterial species were prepared at 50 mg mL^{-1} and

Step-I

$C_6H_9N_2O_6P$ (236) $\xrightarrow{150–190\ °C}$ $C_6H_7N_2O_5P$ (218) + H_2O (18)

Step-II

$C_6H_7N_2O_5P$ (218) $\xrightarrow{190–210\ °C}$ $C_6H_4O_3$ (124) + 2NO (60) + PH_3 (34)

Step-III

$C_6H_4O_3$ (124) $\xrightarrow{210–220\ °C}$ C_4H_4O (68) + 2CO (56)

Note: The values given in parenthesis stand for the molecular weights of the respectipve species.

Fig. 7. Decomposition steps of 3-nitroanilinium dihydrogen phosphate (3NADP)

100 mg mL^{-1} concentrations and the zone of inhibition measured (diameter) of these microorganisms are shown in Table-6. From the results, it was clear that the synthesized 3-nitroanilinium dihydrogen phosphate was moderately active against all the microorganisms.

Conclusions

A bioactive material, 3-nitroanilinium dihydrogen phosphate was synthesized from 3-nitroaniline and orthophosphoric acid. The single crystal of 3NADP was grown by the solvent evaporation solution growth technique. The density and the unit cell constants were determined by X-ray diffraction technique. The FT-IR and FT-Raman spectral data established the molecular structure of 3NADP successfully. Thermal analysis confirmed the absence of phase transition before the material reached the melting point. The low energy gap value from HOMO-LUMO study facilitates the charge delocalization in the title compound, which makes the material to be bioactive. Mulliken charge analysis confirmed the charge distribution occurs between the molecules. From the antimicrobial activities, 3NADP acted as moderately active against the studied microorganisms.

CONFLICT OF INTEREST

The authors declare that there is no conflict of interests regarding the publication of this article.

REFERENCES

1. H. Reis, M.G. Papadopoulos, P. Calaminici, K. Jug and A.M. Köster, *Chem. Phys.*, **261**, 359 (2000); https://doi.org/10.1016/S0301-0104(00)00305-0
2. V. Siva, M. Suresh, S. Athimoolam and S.A. Bahadur, *Acta Crystallogr.*, **E75**, 1627 (2019); https://doi.org/10.1107/S2056989019012957

TABLE-6
ANTIBACTERIAL AND ANTIFUNGAL ACTIVITY OF 3NADP COMPOUND AGAINST SOME HUMAN PATHOGENS

Sample	Concentration (mg/mL)	Zone of inhibition (diameter) (mm)		
		Antibacterial activity		Antifungal activity
		K. neumoniae (Gram-positive)	*S. aureus* (Gram-negattive)	*C. albicans*
3NADP	50	12	Resistant	13
	100	12	Resistant	13
SD	50/100	16	18	16

SD-Standard drug (Antibacterial activity = Amikacin; Antifungal activity = Ketokonazole)

3. V. Krishnakumar and R. Nagalakshmi, *Cryst. Growth Des.*, **8**, 3882 (2008); https://doi.org/10.1021/cg070548i
4. S. Thangarasu, S. Athimoolam and S.A. Bahadur, *Acta Crystallogr.*, **E67**, o2124 (2011); https://doi.org/10.1107/S1600536811029072
5. V. Siva, S. Suresh Kumar, M. Suresh, M. Raja, S. Athimoolam and S.N.-H. Asath Bahadur, *J. Mol. Struct.*, **1133**, 163 (2017); https://doi.org/10.1016/j.molstruc.2016.11.088
6. A. Anandhan, C. Sivasankari, M. Saravanabhavan, V. Siva and K. Senthil, *J. Mol. Struct.*, **1203**, 127400 (2020); https://doi.org/10.1016/j.molstruc.2019.127400
7. S. Premkumar, A. Jawahar, T. Mathavan, M.K. Dhas, V.G. Sathe and A.M.F. Benial, *Spectrochim. Acta A Mol. Biomol. Spectrosc.*, **129**, 74 (2014); https://doi.org/10.1016/j.saa.2014.02.147
8. V. Siva, A. Shameem, A. Murugan, S. Athimoolam, M. Suresh and S.A. Bahadur, *J. Mol. Struct.*, **1205**, 127619 (2020); https://doi.org/10.1016/j.molstruc.2019.127619
9. W.I.F. David, K. Shankland, J. van de Streek, E. Pidcock, W.D.S. Motherwell and J.C. Cole, *J. Appl. Cryst.*, **39**, 910 (2006); https://doi.org/10.1107/S0021889806042117
10. M.J. Frisch, G.W. Trucks, H.B. Schlegel, G.E. Scuseria, M.A. Robb, J.R. Cheeseman, G. Scalmani, V. Barone, B. Mennucci, G.A. Petersson, H. Nakatsuji, M. Caricato, X. Li, H.P. Hratchian, A.F. Izmaylov, J. Bloino, G. Zheng, J.L. Sonnenberg, M. Hada, M. Ehara, K. Toyota, R. Fukuda, J. Hasegawa, M. Ishida, T. Nakajima, Y. Honda, O. Kitao, H. Nakai, T. Vreven, J.A. Montgomery Jr., J.E. Peralta, F. Ogliaro, M. Bearpark, J.J. Heyd, E. Brothers, K.N. Kudin, V.N. Staroverov, R. Kobayashi, J. Normand, K. Raghavachari, A. Rendell, J.C. Burant, S.S. Iyengar, J. Tomasi, M. Cossi, N. Rega, J.M. Millam, M. Klene, J.E. Knox, J.B. Cross, V. Bakken, C. Adamo, J. Jaramillo, R. Gomperts, R.E. Stratmann, O. Yazyev, A.J. Austin, R. Cammi, C. Pomelli, J.W. Ochterski, R.L. Martin, K. Morokuma, V.G. Zakrzewski, G.A. Voth, P. Salvador, J.J. Dannenberg, S. Dapprich, A.D. Daniels, Ö. Farkas, J.B. Foresman, J.V. Ortiz, J. Cioslowski and D.J. Fox, Gaussian, Inc., Wallingford CT, 2009.
11. R.G. Parr and W. Yang, Density-Functional Theory of Atoms and Molecules, Oxford University Press: New York (1989).
12. W. Koch and M.C. Holthausen, A Chemist's Guide to Density Functional Theory, Wiley-VCH: Weinheim, Eds.: 2 (2000).
13. D. Young, Computational Chemistry: A Practical Guide for Applying Techniques to Real World Situations; Wiley-Interscience: New Jersey (2001).
14. R. Dennington, T. Keith and J. Millam, Gauss View, Version 5.0.8, R. KS: Dennington, Semichem Inc., Shawnee Mission (2009).
15. V. Siva, A. Shameem, A. Murugan, S. Athimoolam, M. Suresh and S.A. Bahadur, *Chem. Data Coll.*, **24**, 100281 (2019); https://doi.org/10.1016/j.cdc.2019.100281
16. S. Thangarasu, S. Athimoolam, S.A. Bahadur and A. Manikandan, *J. Nanosci. Nanotechnol.*, **18**, 2450 (2018); https://doi.org/10.1166/jnn.2018.14387
17. S. Thangarasu, S.S. Kumar, S. Athimoolam, B. Sridhar, S. Asath Bahadur, R. Shanmugam and A. Thamaraichelvan, *J. Mol. Struct.*, **1074**, 107 (2014); https://doi.org/10.1016/j.molstruc.2014.05.054
18. G. Sivaraj, N. Jayamani and V. Siva, *J. Mol. Struct.*, **1216**, 128242 (2020); https://doi.org/10.1016/j.molstruc.2020.128242
19. P. Karthiga Devi and K. Venkatachalam, *J. Mater. Sci. Mater. Electron.*, **27**, 8590 (2016); https://doi.org/10.1007/s10854-016-4877-7
20. R. Mathammal, N. Sudha, L.G. Prasad, N. Ganga and V. Krishnakumar, *Spectrochim. Acta A Mol. Biomol. Spectrosc.*, **137**, 740 (2015); https://doi.org/10.1016/j.saa.2014.08.099
21. Z. Demircioglu, A.E. Yesil, M. Altun, T. Bal-Demirci and N. Özdemir, *J. Mol. Struct.*, **1162**, 96 (2018); https://doi.org/10.1016/j.molstruc.2018.02.093
22. N. Prabavathi, A. Nilufer and V. Krishnakumar, *Spectrochim. Acta A Mol. Biomol. Spectrosc.*, **114**, 449 (2013); https://doi.org/10.1016/j.saa.2013.05.011
23. N. Bhuvaneswari, N. Priyadharsini, S. Sivakumar, K. Venkatachalam and V. Siva, *J. Therm. Anal. Calorim.*, **136**, 411 (2019); https://doi.org/10.1007/s10973-018-7908-1
24. V. Krishnakumar, N. Jayamani and R. Mathammal, *J. Raman Spectr.*, **40**, 936 (2009); https://doi.org/10.1002/jrs.2203
25. L.M. Novena, S.S. Kumar, S. Athimoolam, K. Saminathan and B. Sridhar, *J. Mol. Struct.*, **1133**, 294 (2017); https://doi.org/10.1016/j.molstruc.2016.11.087